Mirror slides for high-sensitivity cell and tissue fluorescence imaging

Eric Le Moal
Université Denis Diderot – Paris VII
UMR 7162 CNRS
Laboratoire Matériaux et Phénomènes Quantiques
and
ESPCI
Laboratoire de Physique du Solide
10 rue Vauquelin
75231 Paris Cedex 05, France
and
UPR 3361 CNRS
Laboratoire de Photophysique Moléculaire
91405 Orsay Cedex, France

Emmanuel Fort
Université Denis Diderot – Paris VII
UMR 7162 CNRS
Laboratoire Matériaux et Phénomènes Quantiques
and
ESPCI
Laboratoire de Physique du Solide
10 rue Vauquelin
75231 Paris Cedex 05, France

Sandrine Lévêque-Fort
UPR 3361 CNRS
Laboratoire de Photophysique Moléculaire
91405 Orsay Cedex, France

Anne Janin
Hideyuki Murata
Université Denis Diderot – Paris VII
UMR 728 INSERM
Laboratoire de Pathologie, Hôpital Saint Louis
1 avenue Claude Vellefaux
75010 Paris, France

Fabrice P. Cordelières
Institut Curie – Section de Recherche
CNRS UMR 146
Plateforme d'Imagerie Cellulaire
Bâtiment 112 – Centre Universitaire
91405 Orsay Cedex, France

Marie-Pierre Fontaine-Aupart
UPR 3361 CNRS
Laboratoire de Photophysique Moléculaire
91405 Orsay Cedex, France

Christian Ricolleau
Université Denis Diderot – Paris VII
UMR 7162 CNRS
Laboratoire Matériaux et Phénomènes Quantiques
and
ESPCI
Laboratoire de Physique du Solide
10 rue Vauquelin
75231 Paris Cedex 05, France

Abstract. Fluorescence microscopy has become the method of choice in the majority of life-science applications. We describe development and use of mirror slides to significantly enhance the fluorescence signal using standard air microscope objectives. This technique offers sufficient gain to achieve high-sensitivity imaging, together with wide field of observation and large depth of focus, two major breakthroughs for routine analysis and high-throughput screening applications on cells and tissue samples.
[DOI: 10.1117/1.2722730]

Keywords: mirror slides; fluorescence microscopy; high-sensitivity imaging.

Paper 06287LR received Oct. 13, 2006; revised manuscript received Jan. 31, 2007; accepted for publication Feb. 17, 2007; published online Apr. 16, 2007.

Fluorescence microscopy has undergone a renaissance in the last decade.[1] The introduction of novel fluorescent markers,[2–4] together with the development of novel microscopy techniques,[5–7] made it possible to study biomolecular interactions directly in living cells and to examine the structure and function of living tissues. The impact of these techniques in biophysics, neuroscience, developmental and cell biology, as well as medical diagnosis has been remarkable. However, many biological and medical applications involve the detection of minute quantities of biomolecules, and are thus limited by the weakness of the signal in common observation conditions. Here, we show that mirror substrates can be used as active substrates to provide a significant signal enhancement (about four-fold) for micrometer-thick biological samples with standard air microscope objectives. Resulting wider field of observation and larger depth of focus are of great interest for cell and tissue imaging.

In bioimaging devices, the usual means to obtain a higher fluorescence signal is to increase the efficiency of light collection, by using microscope objectives of large numerical aperture (NA). This latter is defined as $NA = n \sin \theta$, where n is the refractive index of the medium between the sample and the objective lens and θ is the half-angle of the light collection cone. The large NA of oil immersion objectives ($n = 1.51$) permits increasing the light collection efficiency by about three-fold as compared to the best air objectives. Oil immersion objectives are, however, available with high magnifications only (typically higher than 40×), thus providing narrow

Address all correspondence to Eric Le Moal, Laboratoire de Physique du Solide, ESPCI, 10 rue Vauquelin, 75231 Paris Cedex 05, France; Tel: +33(0)1 40 79 47 94; Fax: +33(0)1 40 79 47 30; E-mail: eric.lemoal@espci.fr

1083-3668/2007/12(2)/024030/5/$25.00 © 2007 SPIE

fields of observation, which constitute a strong limitation in a number of biological studies. In tissue imaging, for instance, wide field observations provide information on the global biological architecture of the sample. These observations, together with the localization of molecules of interest inside the cells, provide an essential correlation link between tissue architecture and cell inner structure. Besides, switching from high to low magnification and scanning the sample appears quite tricky because of the oil. Furthermore, the use of high-NA microscope objectives is all the more detrimental in that the high lateral resolution offered by these objectives is in many cases not needed.

Another crucial parameter in cell imaging is the depth of field d_{tot}, which corresponds to the range of depth within which a specimen is in acceptable focus. d_{tot} is related to the NA and to the objective magnification M by the formula $d_{\mathrm{tot}}=\lambda_0 n/\mathrm{NA}^2+ne/(M\cdot\mathrm{NA})$, where λ_0 is the wavelength of illuminating light.[8] The first term depends only on the collection optical geometry, while the second term is associated with the detection device resolution e. Increasing NA or magnification results in a decrease of the depth of field.[9] For instance, the depth of field associated with a $100\times$ NA 1.4 microscope objective is $d_{\mathrm{tot}}\simeq 0.6\ \mu$m, which is about ten times smaller than that of a $20\times$ NA 0.40 objective ($d_{\mathrm{tot}}\simeq 5\ \mu$m). The profiles of biological samples like tissues or cells typically cover a larger range than the depths of field of high NA objectives, and parts of the specimen that lie outside the object plane appear as a blurry contribution on the image of the observed focal plane. Using objectives with high NA and therefore low depths of field, one will consequently need to continuously focus up and down to probe the whole layer of a thick specimen. This is penalizing for large-scale applications like medical diagnosis, and it also substantially complicates and slows down automation for high-throughput screening.

The use of mirror slides permits overcoming these limitations in the case of cell and tissue imaging. Until now, the use of fluorescence-enhancing substrates was limited to biosensing applications and, in particular, to microarray biochips.[10,11] Commercially available "active" slides for such applications are designed to enhance the signal at the very surface of the substrate. In the case of plasmonic-based slides, the enhancement effect is confined to distances of a few tens of nanometers from the surface.[10] For mirror-based slides, a precise tuning of the light phase (for a given wavelength) is needed and obtained by using a quarter-wave spacer layer.[11] Initially, these substrates were not designed to be used for micrometer-thick biological samples. However, we show that simple microscope slides coated with a thin metallic mirror layer provide efficient active substrates for this kind of samples (without needing to use a spacer layer).

We prepared such mirror slides under high vacuum conditions (10^{-8} torr) on conventional coverslips or microscope slides. After standard cleaning procedures (ethanol baths sonicated for 5 min and oxygen plasma cleaning), a metallic thin layer of gold or silver was deposited by thermal evaporation (rate 1 nm/min). An underlayer of chromium or platinum of thickness between 1 and 3 nm was necessary to increase the wetting of gold or silver on the glass substrate and ensure adherence of the metallic thin film. The typical thickness of the metal layer was 50 nm, so as to reach sufficient reflectivity (reflection coefficient $>90\%$ for $\lambda>450$ nm) and to ensure sufficient light transmission for transmission imaging of stained samples. An additional cover layer could also be added to protect the mirror layer and ensure biocompatibility, endowing the mirror substrate surface with chemical properties similar to standard glass. In this work, the thin metal films were covered with a thin layer of amorphous alumina (5 nm) deposited by *pulsed laser deposition* (PLD). The alumina coating ensures cell viability without any additional chemical treatment. Also, no long-term damage has been observed. The morphological characteristics of the substrates were measured using *atomic force microscopy* (AFM). The root-mean-square average roughness of the metallic surface is found to be $R_q=3$ nm. Remarkably, the mirror slides that are developed and commercialized for the *surface plasmon resonance* (SPR) technique can directly be used as active mirror slides for fluorescence imaging of thick biological samples. Note that the metallic thin films are thin enough (typical thickness 40 to 60 nm) to permit transmission observation.

The enhancement of the fluorescence signal can be ascribed to two complementary processes.[12] First, the reflection of the excitation light on the mirror substrate induces an enhancement of the excitation field, which basically contributes a mean factor of 2 to fluorescence enhancement (considering the effective reflectivity of the mirror thin film, the calculated enhancement factor was higher than 1.8 over the entire spectrum). It is also important to note that the incident and reflected beams interfere, resulting in a standing wave pattern with nodes associated to weak excitation of the fluorophores. This phenomenon is expected to be detrimental, since detection is reduced for particular substrate distances. However, no spatial modulation was found in our experimental results. Incident light scattering, surface corrugation, and low-coherence illumination might contribute to partly reduce this modulation.

Second, the emitted light is redirected by the mirror substrate, toward the objective lens, thus increasing the collection efficiency. The latter enhancement, however, depends on the distance between the fluorophore and the slide. When deposited on a standard microscope slide, a fluorophore emits between 68 and 77% of its fluorescence toward the glass slide, because of its near-field coupling.[13] The range of this interaction is limited to distances typically smaller than one hundred nanometers. Thus, particularly large enhancements (typically by a factor 4) can be achieved in this distance range. For larger separation distances, the emission is isotropic on average. Consequently, the redirection of the emitted light improves the collection efficiency more modestly; nevertheless, typical enhancements by a factor of 2 are observed.

The vicinity of a mirror surface also modifies the fluorophore local environment, resulting in changes in its radiative decay rate.[14] This effect raises or lowers the quantum yield, depending on the fluorophore-to-mirror distance, and tends to cancel itself out when averaged over micrometers.

To evaluate the influence of the mirror substrate on the fluorophore, we have used a semiclassical approach, which considers a fluorescing molecule as an ideal dipole emitter.[15] The theoretical description of the emission of dipole emitters, first developed by Sommerfeld,[16] was more recently applied

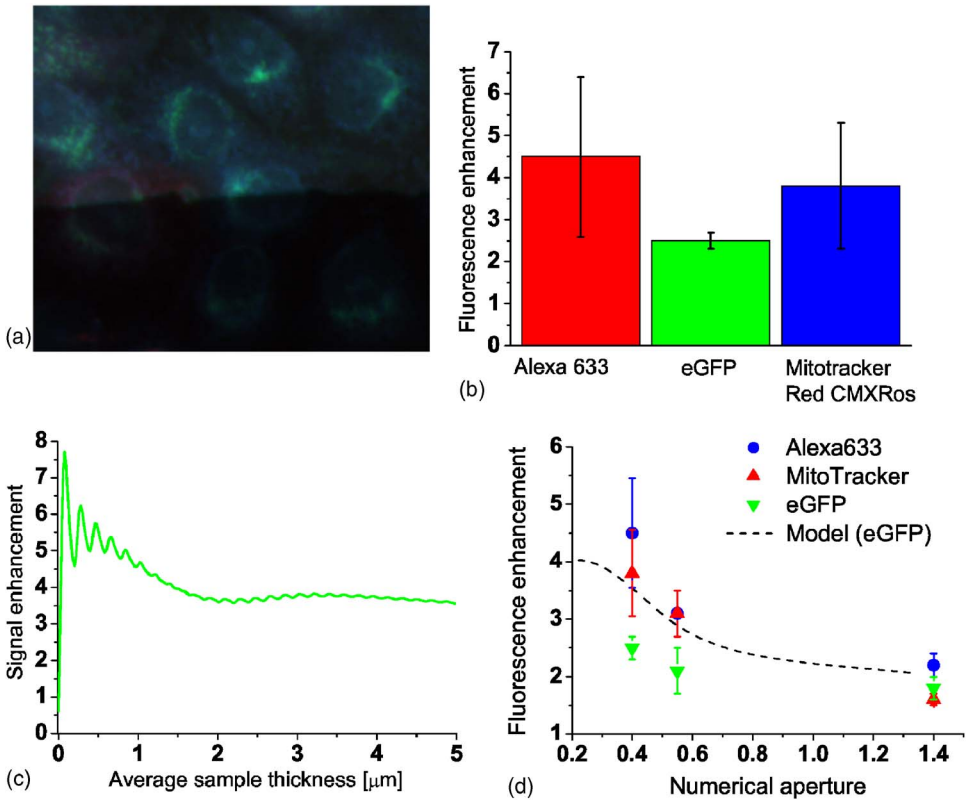

Fig. 1 Application of mirror slides to cell imaging: comparison between standard slide and mirror slide. (a) Closeup of a wide field image of multicolored tagged dog kidney cells deposited on a standard glass slide (bottom) and on a mirror slide (top). The magnification is 200-fold with 20×NA 0.4 air objective. Cell microtubules were tagged with eGFP; Golgi networks with Alexa 633 dyes; and mitochondria with Mitotracker Red CMXRos mitochondrial probes. A set of specific filter cubes was used to image each fluorescent marker channel: Leica L5 (excitation filter BP 480/40 nm, dichroic mirror 505 nm, barrier filter BP 527/30 nm); Leica N3 (excitation filter BP 546/12 nm, dichroic mirror 565 nm, barrier filter BP 600/40 nm); and Leica Y5 (excitation filter BP 620/60 nm, dichroic mirror 660 nm, barrier filter BP 700/75 nm). (b) Experimentally measured signal enhancement for the three fluorophores. (c) Calculated signal enhancement for various sample thicknesses with a NA 0.4 microscope objective. Fluorophores have been modeled with characteristics similar to that of eGFP: excitation wavelength $\lambda_{exc}=489$ nm; emission wavelength $\lambda_{em}=508$ nm; fluorescence quantum yield $Q=0.6$. The fluorophores are assumed to be homogeneously distributed in the sample. Note that the simulations give very similar results for other fluorophore characteristics. (d) Experimental signal enhancements for the three used fluorophores versus microscope objective NA, together with the calculated enhancements (using the parameters of eGFP fluorophore) in a 5-μm-thick sample. Small discrepancies between the modeled and the experimental enhancements originate in the inhomogeneous distribution of the fluorophores in the biological sample.

to the context of molecular emission.[17] This model permits an easy calculation of the power emitted by the molecule into a given solid angle. This is a core quantity required for calculating the optical properties of interest here, like the spatial radiation patterns or the signal enhancement in the presence of a mirror substrate.

In the following, we present two applications on cell cultures and tissue sections that exemplify the need for such active substrates in thick sample imaging.

We first applied our method to fluorescence imaging of dog kidney cells, which are model subjects for the study of subcellular structures within epithelial cells, especially in the context of cancer research.[18] Investigations on epithelium degeneration generally involve statistical studies to evaluate the proportion of cells that exhibits an abnormal inner structure. Such studies require both wide field (low magnification) to get a large reliable statistical population and high contrast (high signal and signal-to-noise ratio) to achieve an accurate diagnosis.

Images of fixed cells were collected using an imaging system described elsewhere.[19,20] Briefly, the setup is made of a Leica DM RXA microscope (Leica Microsystems GmbH, Wetzlar, Germany), equipped with a 100× PlanAPO NA 1.4 oil immersion objective positioned by a PIFOC piezoelectric translator (Physik Instrumente, Karlsruhe, Germany). Two air objective lenses (40×NA 0.55 and 20×NA 0.4) were additionally used with the aim of demonstrating the collection efficiency improvement on metal-coated substrates. A 5-MHz Micromax 1300Y interline charge-coupled device (CCD) camera (Roper Instruments, Trenton, New Jersey) was used to collect fluorescence images, the full system being under the control of Metamorph software (Molecular Devices, Wokingham, United Kingdom).

Figure 1(a) shows a fluorescence image that illustrates the enhancement of both the signal intensity and the image contrast, on a mirror slide (top) as compared to a standard microscope slide (bottom). The images represent details of wide

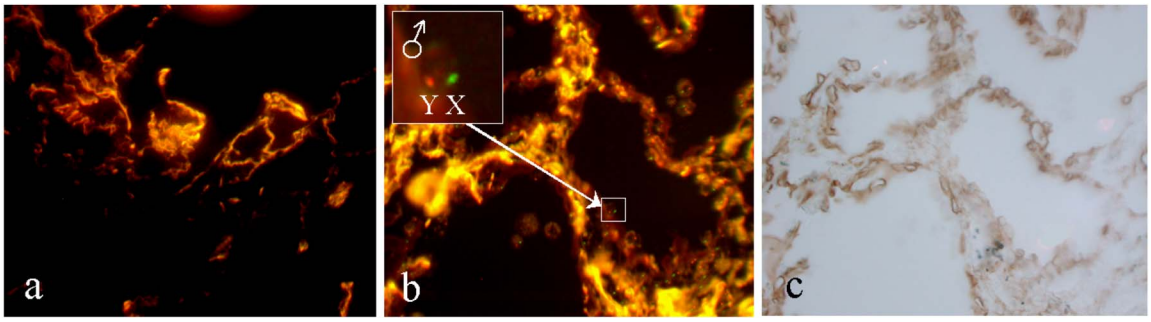

Fig. 2 Application of mirror slides to tissue imaging for medical diagnosis. Fluorescence *in situ* hybridization (FISH) is performed to identify the X- or Y-chromosome together with immunologic staining to characterize cell types on the same tissue section. Fluorescence images of the same tissue section, from a biopsy made on a human lung graft (transplanted from a female donor to a male recipient), on (a) a standard microscope slide and (b) on a mirror slide (c) Transmission image of the stained section on the same observation field as (b). The cut is formalin-fixed and paraffin-embedded. Its thickness is 5 μm. FISH protocol: acid pretreatment: 0.2-M HCl for 15 min; heat treatment: 2× SSC at 80°C for 15 min; enzymatic treatment: digestion, proteinase K (100 g/mL) in TEN buffer at 37°C for 15 min; denaturation at 90°C for 20 min on heating plate; hybridization at 42°C for 16 h in moist chamber. DNA probes: CEP X (excitation wavelength 500 nm, emission wavelength 530 nm); CEP Y (excitation wavelength 560 nm, emission wavelength 590 nm). The images are obtained with a magnification of 400-fold using a 40×NA 0.4 microscope objective. Cubes: Olympus U-MWIB (excitation filter 460 to 490 nm, dichroic mirror 505 nm, barrier filter 515 nm); Olympus U-MWIG (excitation filter 520 to 550 nm, dichroic mirror 565 nm, barrier filter 580 nm).

field images obtained with a 20×NA 0.4 microscope objective. In the present case, a multicolored immunolabeling was used to visualize the various relevant biological structures (*e.g.*, green for microtubules and red for mitochondria). Signal intensity was found to be amplified by about a factor of 4 on mirror slides. Remarkably, the mirror substrates provide a significant enhancement on the entire visible range, thus enabling multicolor tagging [see Fig. 1(b)]. Image contrast is defined as the signal-to-noise ratio, where the noise level is measured in areas without biological material. On metal-coated slides, the contrast is found to be increased by a factor of 1.5. Using the dipole model described earlier, the average detected light can be calculated for various sample thicknesses and various NA [see Figs. 1(c) and 1(d)]. Both theoretical and experimental results verify that mirror slides are of particular interest to improve detection sensitivity with low-NA objectives. The difference between the enhancement factors of the fluorophores is due to their inhomogeneous distribution in the biological sample due to their specific tagging. This variation is not related to the spectral response of the mirror slides, which reflects more than 90% of the light over the entire visible spectrum. Note that the discrepancies between theoretical and experimental enhancement factors also originate from the inhomogeneous distribution of the fluorophores in the sample.

In a second application, we applied mirror slides to tissue imaging for medical diagnosis, in the follow-up of the microvessel repair in sex-mismatched human grafts. In a series of biopsies, performed for diagnostic purpose in female lungs transplanted in male recipients, genotype analysis of endothelial cells was performed to determine the origin (donor or recipient) of endothelial cells involved in microvessel repair of the transplanted lung. To do so, we combined X- and Y-chromosome detection by fluorescence *in situ* hybridization (FISH) with immunohistochemical staining.[21]

FISH involved CEP X and CEP Y DNA probes for chromosome X and chromosome Y, respectively. For immunohistochemistry, we used mouse antihuman CD34 antibody (endothelial cell and hematopoietic progenitor cell marker), and Peroxidase/DAB (3,3-diaminobenzidine tetrahydrochloride). Images of tissue section were collected using an Olympus AX70 microscope (Olympus Europe, Hamburg, Germany), equipped with a 40× air objective (total magnification: 400×).

Figure 2 shows fluorescence images of the same tissue section on a standard microscope slide [Fig. 2(a)] and on a mirror slide [Fig. 2(b)]. While the donor (XX) or recipient (XY) origin of the cells is impossible to determine on the standard slide owing to signal weakness, it appears readily on the mirror slide (see inset close up), together with the necessary link with the tissue structure, thanks to fluorescence enhancement. This way, we characterized the endothelial cells and their genotype on the same tissue section, and we established that the presence of endothelial cells of recipient origin was correlated with graft rejection. This example highlights two major technological needs in medical applications for day-to-day diagnosis. On the one hand, wide field imaging is necessary for histologic diagnosis, since it implies the examination of the global tissue architecture. On the other hand, high collection efficiency is needed for genotype analysis, which is based on the detection of weak signals from fluorescent probes bounded to X and Y chromosomes. To achieve a complete and accurate diagnosis, it is thus necessary to switch several times from a low-magnification air microscope objective to a high-magnification oil immersion one. The latter task is not easy, because of the presence of oil, and time consuming, which is a major drawback because of fluorescence signals gradual fading due to photodestruction. We demonstrate that such microscope objectives are not required anymore when using mirror slides. The latter slides indeed provide sufficient sensitivity and contrast at low magnification to achieve widefield imaging of the chromosomes, allowing one to simultaneously image the tissue architecture [see Figs. 2(a) and 2(b)]. It is noteworthy that standard transmission imaging of the stained tissues remains possible on the mirror slides over the entire visible spectrum [see Fig. 2(c)] thanks to nonzero optical transmission (although only a small part of the light is

transmitted). This technique thus allows one to compare histological and immunofluorescence information, on the same section, with a single low-magnification objective. As a result, high-throughput screening can be achieved, which is a strong advantage in a clinical context.

In summary, mirror substrates provide an elegant means of enhancing the fluorescence signal over sample thicknesses of a few micrometers. They permit reaching sufficient signal sensitivity for many biological and medical applications using low-NA microscope objectives. Thus, when high resolution is not needed, one can keep a low magnification to simultaneously image a large field of observation with a high depth of field, which is essential for imaging of thick samples such as cells and tissues.

Acknowledgment

This work was supported by the French research ministry and the National Center for Scientific Research (CNRS) through the Nanoscience-Nanotechnology program.

References

1. J. W. Lichtman and J. A. Conchello, "Fluorescence microscopy," *Nat. Methods* **2**(12), 910–919 (2005).
2. J. Lippincott-Schwartz and G. H. Patterson, "Development and use of fluorescent protein markers in living cells," *Science* **300**(5616), 87–91 (2003).
3. C. Seydel, "Quantum dots get wet," *Science* **300**(5616), 80–81 (2003).
4. J. K. Jaiswal, H. Mattoussi, J. M. Mauro, and S. M. Simon, "Long-term multiple color imaging of live cells using quantum dot bioconjugates," *Nat. Biotechnol.* **21**(1), 47–51 (2003).
5. D. J. Stephens and V. J. Allan, "Light microscopy techniques for live cell imaging," *Science* **300**(5616), 82–86 (2003).
6. J. A. Conchello and J. W. Lichtman, "Optical sectioning microscopy," *Nat. Methods* **2**(12), 920–931 (2005).
7. D. Axelrod, "Total internal reflection fluorescence microscopy in cell biology," *Traffic (Oxford, U. K.)* **2**(11), 764–774 (2001).
8. S. Inoue and R. Oldenbourg, "Microscopes," in *Handbook of Optics*, 2nd eds., McGraw-Hill, New York (1995).
9. P. Perlman, *Basic Microscope Techniques*, Chap. 1, p. 24, Chemical Publishing Company, New York (1971).
10. C. Mayer, N. Stich, T. Schalkhammer, and G. Bauer, "Slide-format proteomic biochips based on surface-enhanced nanocluster-resonance," *Fresenius' J. Anal. Chem.* **371**(2), 238–245 (2001).
11. H. Choumane, N. Ha, C. Nelep, et al., "Double interference fluorescence enhancement from reflective slides: Application to bicolor microarrays," *Appl. Phys. Lett.* **87**, 031102 (2005).
12. E. Le Moal, E. Fort, S. Lévêgue-Fort, F. P. Cordelières, M.-P. Fontaine-Aupart, and C. Ricolleau, "Enhanced fluorescence cell imaging with metal-coated slides," *Biophys. J.* **92**(6), 2150–2161 (2007).
13. J. Enderlein, "Single-molecule fluorescence near a metal layer," *Chem. Phys.* **247**(1), 1–9 (1999).
14. W. L. Barnes, A. Dereux, and T. W. Ebbesen, "Surface plasmon subwavelength optics," *Nature (London)* **424**(6950), 824–830 (2003).
15. R. R. Chance, A. Prock, and R. Silbey, "Lifetime of an emitting molecule near a partially reflecting surface," *J. Chem. Phys.* **60**, 2744–2748 (1974).
16. A. Sommerfield, *Partial Differential Equations in Physics*, Academic Press, New York (1949).
17. G. W. Ford and W. H. Weber, "Electromagnetic interactions of molecules with metal surfaces," *Phys. Rep.* **113**(4), 195–287 (1984).
18. J. M. Vasiliev, T. Omelchenko, I. M. Gelfand, H. H. Feder, and E. M. Bonder, "From the cover: Rho overexpression leads to mitosis-associated detachment of cells from epithelial sheets: A link to the mechanism of cancer dissemination," *Proc. Natl. Acad. Sci. U.S.A.* **101**(34), 12526–12530 (2004).
19. T. M. Savino, J. Gebrane-Younes, J. De Mey, J.-B. Sibarita, and D. Hernandez-Verdun, "Nucleolar assembly of the rRNA processing machinery in living cells," *J. Cell Biol.* **153**(5), 1097–1110 (2001).
20. J. B. Sibarita, H. Magnin, and J. De Mey, "Ultra-fast 4D microscopy and high throughput distributed deconvolution," *Proc. IEEE Int. Symp. Biomed. Imaging*, 769–772 (2002).
21. V. Meignin, J. Soulier, F. Brau, M. Lemann, E. Gluckman, A. Janin, and G. Socie, "Little evidence of donor-derived epithelial cells in early digestive acute graft-versus-host disease," *Blood* **103**(1), 360–362 (2004).